

# High Efficiency Silicon Strip Waveguide to Plasmonic Slot Waveguide Mode Converter

Chin-Ta Chen<sup>a,b</sup>, Xiaochuan Xu<sup>c</sup>, Amir Hosseini<sup>c</sup>, Zeyu Pan<sup>a</sup>, and Ray T. Chen<sup>a,c\*</sup>

a. Department of Electrical and Computer Engineering, University of Texas at Austin, Austin, Texas 78758, USA

b. Department of Optics and Photonics, National Central University, Jhongli 32001, Taiwan;

c. Omega Optics, Inc., Austin, Texas 78757, USA;

\*Corresponding: raychen@uts.cc.utexas.edu

## ABSTRACT

A high-efficiency silicon strip waveguide to plasmonic slot waveguide converter based on the hybrid silicon-gold taper is proposed and optimized. Through investigating the mode matching, the effective index matching, and the metallic absorption loss considerations, the hybrid silicon-gold taper with an overall length of 1.7  $\mu\text{m}$  having a very high conversion efficiency of 93.3% at 1550nm is achieved. Besides, the configuration limitations for restricting this mode converter to achieve a 100 % conversion efficiency are also studied in this paper. Such a high efficiency converter will be an essential component in ultra-compact integrated circuits.

**Keywords:** photonic integrated circuit, surface plasmons, nanophotonics

## 1. INTRODUCTION

Plasmonic devices enable linear and non-linear processing of light beyond the diffraction limit [1], and thus have drawn considerable attention in recent years. Several plasmonic waveguide structures such as metallic nanoparticle arrays and metallic nanowires have been proposed, but most of them only support highly confined modes near the surface plasmon frequency [14]. A metal-insulator-metal (MIM) waveguide structure supports nanometer-size modes over a wide wavelength range and therefore, is more interesting for applications including optical waveguides [6]-[15], light sources [2], detectors [3], and modulators [4], [5], etc. However, due to the high propagation loss ( $>1$  dB/ $\mu\text{m}$ ) [8], [11], [12], MIM waveguides must be made as short as possible. An ideal system would exploit MIM structures as subwavelength optoelectronic devices and utilize conventional dielectric waveguides to carrier the signal over distances longer than a few tens of micronmeter. Efficient dielectric-to-plasmonic slot waveguide couplers will therefore be of significant importance.

To realize low loss coupling, various coupler structures have been investigated, including a taper-funnel coupler with a theoretical efficiency of 33 % (300-nm-wide silicon waveguide to 200-nm-wide MIM waveguide) [10], a silicon-gold plasmonic coupler with a theoretical efficiency of 88 % (450-nm-wide silicon waveguide to 200-nm-wide MIM waveguide) [11], a silicon slot waveguide with a theoretical efficiency of about 70 % (silicon slot waveguide with a slot width of 120 nm to quasi-plasmonic slot waveguide) [12], an air-gap coupler with 88 % efficiency (300-nm-wide silicon waveguide to 40-nm-wide MIM waveguide) [13], a multisection taper with a 2D theoretical efficiency of 93 % (300-nm-wide silicon waveguide to 50-nm-wide MIM waveguide) [14], etc. Although these tapers show great promise, none of these could achieve zero loss conversion theoretically. An investigation on the root cause of the conversion loss would give some clues on how to increase the coupling efficiency even further, which is the focus of this paper.

The discussion is organized as follows. First, the proposed mode converter geometry and simulation configurations are described. The evolution of plasmonic slot waveguide mode within the hybrid silicon-gold taper is investigated in order

to understand the root cause of conversion loss. Then, we study the configuration of hybrid silicon-gold taper from three aspects of mode matching, effective index matching, and metallic absorption loss. The configuration limitations for the hybrid silicon-gold taper that would possibly restrict the mode converter to achieve a near 100 % conversion efficiency are also discussed. According to the above-mentioned discussions, a mode converter design providing conversion efficiency up to 93.3 % at 1550 nm is presented.

## 2. DESIGN AND CONFIGURATION OF MODE CONVERTER

The dielectric-to-plasmonic slot waveguide mode converter based on a hybrid silicon-gold taper is shown in Fig. 1 (a). Figure 1 (b-d) shows the cross sections of (b) a silicon strip waveguide with the waveguide width of 450 nm and height of 250 nm, (c) a hybrid silicon-gold taper, and (d) a plasmonic slot waveguide with the metal height of 250 nm and the slot width of 250 nm. The SU8 thickness above the metal is 1.5  $\mu\text{m}$ .

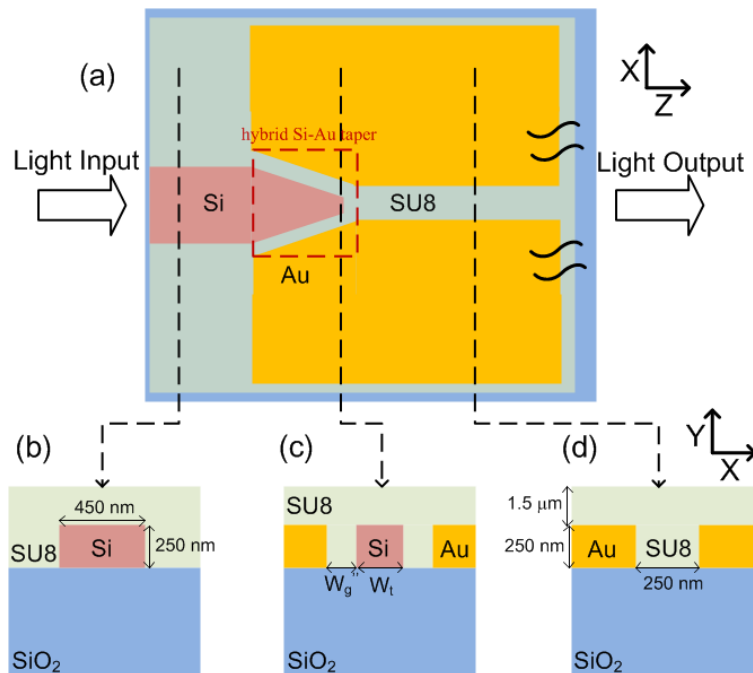


Figure 1. Schematic diagrams of dielectric-to-plasmonic slot waveguide mode converter based on a hybrid silicon-gold taper. (a) Top view of the mode converter with a silicon strip waveguide at the input and a plasmonic metal slot waveguide at the output. Cross sections of (b) a silicon strip waveguide, (c) a hybrid silicon-gold taper, and (d) a plasmonic slot waveguide.

The dielectric-to-plasmonic slot waveguide mode converter is studied with three-dimensional (3-D) finite-difference time-domain (FDTD) simulations. At the operating wavelength of 1550 nm, the material refractive indices of silicon (Si), SiO<sub>2</sub>, SU8, and gold (Au) are 3.476, 1.45, 1.575, and 0.55+i11.5, respectively. The conversion efficiency of mode converter is defined as the ratio of the power coupled into the plasmonic slot waveguide mode to the input power in the silicon waveguide. Power coupled into the plasmonic slot waveguide mode is estimated by monitoring the output of the plasmonic slot waveguide and subtracting the propagation loss of plasmonic slot waveguide.

Mode matching, effective index matching and metal absorption in this structure and the tradeoffs among them for maximizing the overall efficiency are discussed below.

## 2.1 Mode Matching

Although it has been theoretically shown by 2D simulation that directly connecting a slab waveguide to a plasmonic slot waveguide could give a 70% coupling efficiency [14], a close match of two optical fields is still the key to high conversion efficiency [12]. Figure 2 (a) shows the field distribution ( $E_x$ ) in the x-z plane, which shows the evolution of the optical mode from the silicon strip waveguide to the plasmonic slot waveguide via a hybrid silicon-gold taper. Considering the practical limitations on fabrication, the silicon taper width at the tip is assumed to be 60 nm in the simulations. Figures 2 (b-f) show the cross-sections of fields at different locations along the mode converter, which are computed using a finite element method (FEM) mode solver. Figures 2 (b) and (f) show the field distributions of the silicon strip waveguide and the plasmonic slot waveguide, respectively. As can be seen, the dielectric and the plasmonic possess large differences in the field distribution. A good mode matching between these two waveguides through a low loss converter will therefore be important.

Figures 2 (c) and (d) show the field distributions at the beginning and at the end of the taper, respectively. The field distribution at taper beginning resembles a strip waveguide mode. The field distribution at taper end becomes a hybrid plasmonic slot waveguide mode [15], which is confined in the gaps between silicon and gold. Lossless transformation from (c) to (d) is realized by narrowing the silicon waveguide tip to less than the diffraction limitation. As shown in the inset of Fig.4, there is a gap (G) between the silicon taper and the plasmonic slot waveguide. Figure 2 (e) shows the mode at the middle of the gap. Figure 2 (f) shows the plasmonic slot waveguide mode, which could be strongly confined within the metallic slot. Through a metallic taper-funnel coupler, Figures 2 (e) and (f) should have similar field distributions. However, in order to achieve a high conversion efficiency, the mode matching at the input and output interfaces of the hybrid silicon-gold taper must be further improved including the interfaces of the silicon strip waveguide and the hybrid silicon-gold taper at taper beginning as well as the hybrid silicon-gold taper and plasmonic slot waveguide.

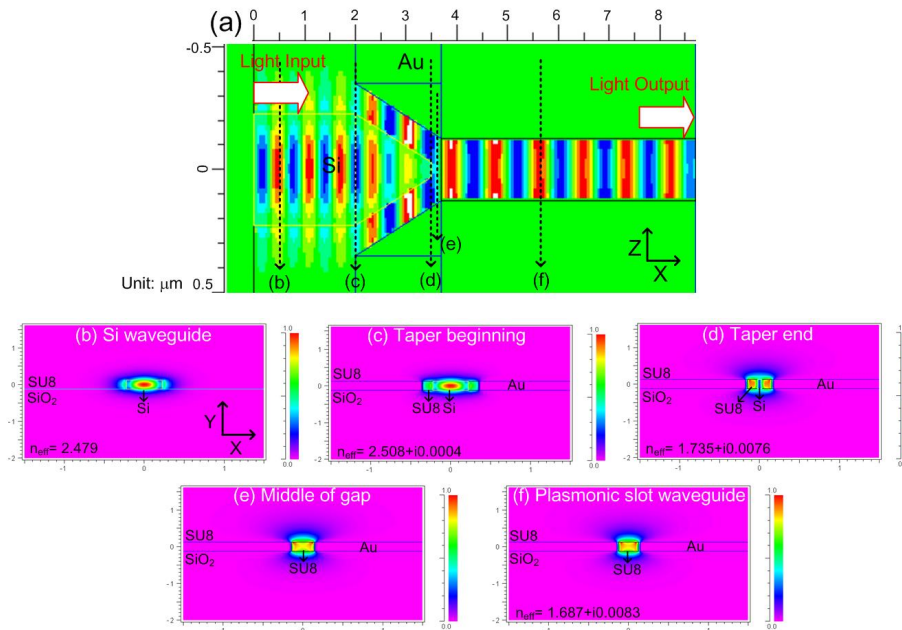


Figure 2. Field distribution ( $E_x$ ) of mode converter at 1550 nm. (a) Top view at the mode converter center. Cross-section views of (b) the silicon strip waveguide, (c) the hybrid silicon-gold taper at the taper beginning, (d) the hybrid silicon-gold taper at the taper end, (e) middle of gap between the silicon taper and the plasmonic slot waveguide, and (f) the plasmonic slot waveguide.

Before looking into mode matching at these interfaces, the alignment of the modes along the y (vertical) direction needs to be discussed in advance. In 2D simulation, the modes are assumed to have a perfect alignment in the y direction, which is not always true. Due to asymmetric claddings along y direction, optical fields tend to shift to the high index region. For example, when air is used as the top cladding material, the plasmonic slot waveguide mode within the hybrid silicon-gold taper and plasmonic slot waveguide will penetrate into the bottom cladding of  $\text{SiO}_2$ , causing an abrupt

variation of the electromagnetic field, as shown in Fig. 3 (a). The problem could be ameliorated by using materials with higher refractive index as the top cladding.

In this paper, SU8 instead of air is chosen to fill in the hybrid silicon-gold taper and plasmonic slot waveguide in order to reduce the coupling loss in the y direction. As shown in Fig. 3 (b), the plasmonic slot waveguide mode is “pulled up” to improve the mode matching with the silicon strip waveguide mode. Ideally, the modes will be perfectly aligned when the material is symmetric along y direction, but in most cases misalignment along y direction exists which compromises the conversion efficiency. For example, a silicon-plasmonic hybrid racetrack ring modulator was discussed in [4]. An electro-optic (EO) polymer as a top cladding having a higher refractive index than a bottom cladding of SiO<sub>2</sub> is filled in the slot of the MIM waveguide to achieve high-speed modulation. Therefore, in order to study the asymmetric cladding along y direction with the mode converter, we choose a common polymer material of SU8 as the top cladding to convert the mode converter. Another benefit from using materials with higher refractive index as a top cladding is the reduction in the propagation loss of the plasmonic slot waveguide. In this case (using SU8 as the top cladding), a propagation loss as small as 0.32 dB/μm could be obtained due to its better guiding capability in the y direction, especially at the SU8/SiO<sub>2</sub> interface.

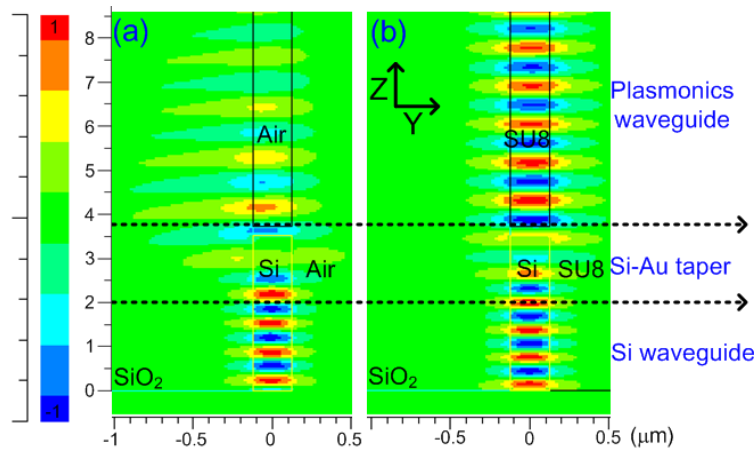


Figure 3. Field distributions of mode converter at waveguide center ( $x=0$ ) using (a) air and (b) SU8 as a top cladding.

As aforementioned, the field distributions in Figs.2 (b) and (c) have apparent differences due to the presence of metal in Fig.2 (c). Although most of light is still confined in silicon, the evanescent wave interacts with metals, which alters the field distribution. Therefore, in order to achieve an effective mode matching, the gap between silicon and gold ( $W_g$ ) needs to be large enough. In this case, we evaluate the conversion efficiencies of the mode converter as a function of metallic taper-funnel angle ( $\theta$ ).  $W_g$  would increase as the  $\theta$  increases. The angle of 7.5 degrees and length of 1.5 μm for the silicon taper,  $G$  of 0.2 μm and the length of metallic taper-funnel coupler (1.7 μm) are fixed in this simulation. The simulation result is shown in Fig. 4. The maximum conversion efficiency of hybrid silicon-gold taper as 93.3 % is obtained at  $\theta = 8.5$  degrees. The efficiency decreases when  $\theta$  is larger than 8.5 degrees. The reason is that a larger taper angle would cause a higher radiation loss. When  $\theta$  is less than 8.5 degrees, the efficiency decreases due to the poor mode matching.

As shown in Figs. 2 (d) and (f), two modes have difference in the field distribution because of the presence and absence of silicon, respectively. In this case, the conversion efficiency of the mode converter is studied by the tuning silicon taper tip width ( $W_t$ ). In this simulation, the angle of 7.5 degrees for the silicon taper, the  $G$  of 0.2 μm, and the angle of 8.5 degrees and length of 1.7 μm for the metallic taper-funnel coupler are fixed. The simulation result is shown in Fig. 5. As expected the highest conversion efficiency of 93.3 % is obtained for a narrow silicon taper tip width (60 nm in our case) and the conversion efficiency will decrease as the silicon taper tip width increases due to the poor mode matching. However, although a narrow taper tip width could enhance the mode matching, it would also cause a higher metallic absorption loss. For example, for an ideal case of taper tip width as 0 μm, the conversion efficiency of only 91.5 % is obtained.

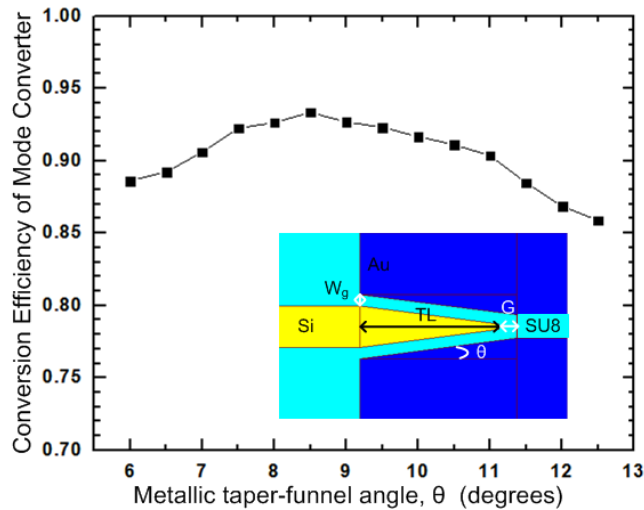


Figure 4. Conversion efficiencies of the mode converter as a function of metallic taper-funnel angle ( $\theta$ ).

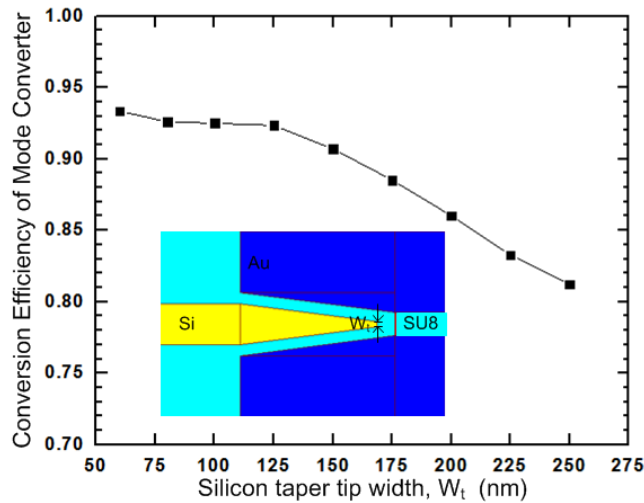


Fig.5. Conversion efficiencies of the mode converter as a function of silicon taper tip width ( $W_t$ ).

## 2.2 Effective Index Matching

Effective index matching between the plasmonic slot waveguide and the hybrid silicon-gold taper is also studied. The effective index of hybrid silicon-gold taper at taper end can be engineered by tuning the gap between silicon and gold ( $W_g$ ) or the silicon taper tip width ( $W_t$ ), as shown in the inset of Fig. 6. Figure 6 shows the real and imaginary parts of effective indices of the hybrid silicon-gold taper at taper end as a function of  $W_g$ . Both the real and imaginary parts of effective indices decreases with increasing  $W_g$ . This suggests that a large  $W_g$  benefits from the effective index matching and also reduces the metallic absorption loss. In this simulation,  $W_t$  is fixed at 60 nm in order to maintain the inclined angle of silicon taper.

The real part of the effective index of plasmonic slot waveguide mode shown in Fig. 2 (f) is 1.684. As shown in Fig. 6, for the metallic taper-funnel angle of 8.5 degrees, its corresponding real part of effective index is 1.735 ( $W_g$ :125 nm). Considering the imperfect effective index matching between the hybrid silicon-gold taper at taper end and the plasmonic slot waveguide, these two modes have an index difference (real part) of about 0.05 caused by a higher refractive index of silicon. Although a lower effective index of hybrid silicon-gold taper could be obtained by increasing the  $W_g$ , a larger  $W_g$  also increases metallic taper-funnel angle that causes a higher radiation loss.

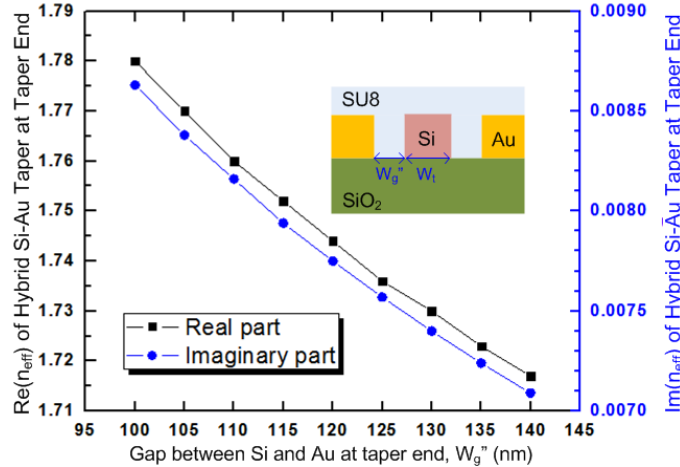


Figure 6. Effective indices of a hybrid silicon-gold taper at taper end as a function of the gap ( $W_g$ ).

### 2.3 Metallic Absorption Loss within the Hybrid Si-Au Taper

Although a hybrid plasmonic slot waveguide mode can be generated through the hybrid silicon-gold taper, the longer hybrid silicon-gold taper the higher metallic absorption loss is. Therefore, the tradeoff between the radiation loss of the silicon taper and the metallic absorption loss within the hybrid silicon-gold taper is studied by optimizing the silicon taper length (TL). In this case, the length of the metallic taper-funnel coupler is varied as the TL is changed. Figure 7 depicts the conversion efficiency of the mode converter as a function of silicon taper length. The mode converter has high conversion efficiencies of more than 85% for different taper length from 1  $\mu\text{m}$  to 3.5  $\mu\text{m}$ . Finally, the highest conversion efficiency of 93.3 % is achieved at a silicon taper length of 1.5  $\mu\text{m}$ . For the taper lengths less than 1.5  $\mu\text{m}$ , the radiation loss of the silicon taper lowers the conversion efficiency. For the taper lengths greater than 1.5  $\mu\text{m}$ , the extra metallic absorption loss decreases the conversion efficiency.

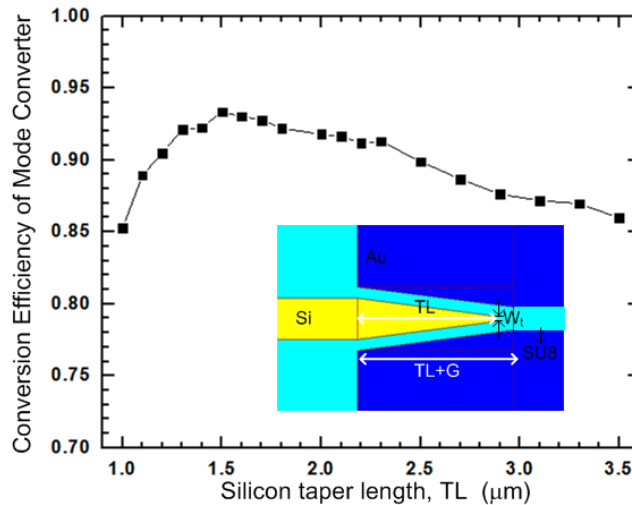


Figure 7. Conversion efficiencies of the mode converter as a function of silicon taper length (TL).

### 3. CONCLUSION

In this paper, based on the mode matching, the effective index matching and the metallic absorption loss considerations, the configuration of hybrid silicon-gold taper with an overall length of 1.7  $\mu\text{m}$  is studied and optimized to achieve the highest conversion efficiency of 93.3 % at 1550nm. The simulation unveils that compromises have to be made between mode/index matching and absorption/radiation loss, and therefore, it is very challenging to achieve 100% conversion efficiency for the mode converter based on the hybrid silicon-gold taper.

### REFERENCES

- [1] D. K. Gramotnev and S. I. Bozhevolnyi, "plasmonics beyond the diffraction limit," *Nature Photon.*, 4, 83-91 (2010).
- [2] K. C. Y. Huang, M.-K. Seo, T. Sarmiento, Y. Huo, J. S. Harris and M. L. Brongersma, "Electrically driven subwavelength optical nanocircuits," *Nature Photon.*, 8, 244-249 (2014).
- [3] S. Zhu, G. Q. Lo, and D. L. Kwong, "Theoretical investigation of silicide Schottky barrier detector integrated in horizontal metal-insulator-silicon-insulator-metal nanoplasmonic slot waveguide," *Opt. Express*, 19(17), 15843-15854 (2011).
- [4] M. Xu, F. Li, T. Wang, J. Wu, L. Lu, L. Zhou, and Y. Su, "Design of an Electro-Optic Modulator Based on a Silicon-Plasmonic Hybrid Phase Shifter," *J. Lightw. Technol.*, 31(8), 1170-1177 (2013).
- [5] A. Melikyan, N. Lindenmann, S. Walheim, P. M. Leufke, S. Ulrich, J. Ye, P. Vincze, H. Hahn, Th. Schimmel, C. Koos, W. Freude, and J. Leuthold, "Surface plasmon polariton absorption modulator," *Opt. Express*, 19(9), 8855-8869 (2011).
- [6] H. Choo, M.-K. Kim, M. Staffaroni, T. J. Seok, J. Bokor, S. Cabrini, P. J. Schuck, M. C. Wu and E. Yablonovitch, "Nanofocusing in a metal - insulator - metal gap plasmon waveguide with a three-dimensional linear taper," *Nature Photon.*, 6, 838-844 (2012).
- [7] A. Melikyan, M. Kohl, M. Sommer, C. Koos, W. Freude, and J. Leuthold, "Photonic-to-plasmonic mode converter," *Opt. Lett.*, 39(12), 3488-3491 (2014).
- [8] R. Yang and Z. Lu, "Silicon-on-Insulator Platform for Integration of 3-D Nanoplasmonic Devices," *IEEE Photon. Technol. Lett.*, 23(22), 1652-1654 (2011).
- [9] Y. Liu, Y. Lai, and K. Chang, "Plasmonic Coupler for Silicon-Based Micro-Slabs to Plasmonic Nano-Gap Waveguide Mode Conversion Enhancement," *J. Lightw. Technol.*, 31(11), 1708-1712 (2013).
- [10] Z. Han, A. Y. Elezzabi, and V. Van, "Experimental realization of subwavelength plasmonic slot waveguides on a silicon platform," *Opt. Lett.*, 35(4), 502-504 (2010).
- [11] J. Tian, S. Yu, W. Yan, and Min Qiu, "Broadband high-efficiency surface-plasmon-polariton coupler with silicon-metal interface," *Appl. Phys. Lett.*, 95, 013504 (2009).
- [12] R. Yang, R. A. Wahsheh, Z. Lu, and M. A. G. Abushagur, "Efficient light coupling between dielectric slot waveguide and plasmonic slot waveguide," *Opt. Lett.*, 35(5), 649-651 (2010).
- [13] R. A. Wahsheh, Z. Lu and M. A. G. Abushagur, "Nanoplasmonic couplers and splitters," *Opt. Express*, 17(21), 19033-19040 (2009).
- [14] G. Veronis and S. Fan, "Theoretical investigation of compact couplers between dielectric slab waveguides and two-dimensional metal-dielectric-metal plasmonic waveguides," *Opt. Express*, 15(3), 1211-1221 (2007).
- [15] J. T. Kim and S. Park, "The Design and Analysis of Monolithic Integration of CMOS-Compatible Plasmonic Waveguides for On-Chip Electronic-Photonic Integrated Circuits," *J. Lightw. Technol.*, 31(18), 2974-2981 (2013).